Intelligent E-Bike Theft Detection Using Interval Type-2 Fuzzy Logic

Meadows O. Ayobami
Smart Systems Engineering
Hanze University of Applied Sciences
Email: oa.meadows@st.hanze.nl

Saman Gharagozlou
Smart Systems Engineering
Hanze University of Applied Sciences
Email: s.gharagozlou@st.hanze.nl

***Abstract*—The widespread adoption of e-bikes has intensified concerns about theft, creating a need for intelligent security solutions capable of distinguishing between legitimate and suspicious bike movements. This project presents a novel Interval Type-2 Fuzzy Logic System (IT2FLS) for theft detection in e-bikes, leveraging accelerometer-derived features including lift acceleration, tilt, pedal stillness, car motion, and z-axis orientation. By applying a fuzzy inference framework that accounts for sensor uncertainty, the system generates a defuzzified theft risk score, enabling distinct differentiation between theft-like behaviour and normal usage such as parking maneuvers. Five realistic scenarios were tested, including both theft and non-theft events, and performance was evaluated using standard metrics and risk score analysis. We also compared our results with those from a Type-1 Fuzzy Logic System (T1FLS). The IT2FLS achieved perfect accuracy by correctly classifying all scenarios, outperforming the T1FLS which showed some misclassifications under the same conditions. These results demonstrate the robustness of IT2FLS as an effective and practical approach for intelligent e-bike theft detection. The complete Python implementation and collected dataset used in this study are publicly available at: github.com/Aysticky/IT2FLS-Ebike-Theft-Detection.**

***Index Terms*—E-bike, theft, fuzzy logic, fuzzy inference, butterworth filter, bouwtag, bypoint.**

I. Introduction

A. Background

Electric bikes, or e-bikes, are one of the fastest-growing parts of the transportation market. Although the first commercial e-bikes were made in Japan in the early 1980s, they did not become popular until the early 2000s because the technology was too limited and expensive before then. Since then, better batteries, motors, and cheaper production have made e-bikes faster, able to travel longer distances, and more affordable than ever before [1].

Today, China sells the most e-bikes in the world, with the Netherlands and Germany following behind. E-bikes make it easier for people to ride because they can keep up speed with less effort. Studies show that e-bikes encourage more people to cycle, improve health, and produce much less carbon dioxide compared to cars traveling the same distance [2].

The Netherlands is famous for being a cycling country. People there love to ride bikes, and electric bicycles have become very popular. In 2019 alone, over 420,000 new e-bikes were sold. But this popularity has a downside: because e-bikes are expensive, they have become a big target for thieves. While the theft of regular bikes has been going down, e-bike theft is rising. Many insurance companies either charge very high prices to insure e-bikes or refuse to cover them at all [3].

A Dutch organization called S.A.F.E., which focuses on bike theft prevention, released a large study showing that current efforts to stop bike theft are not working well. It found that not only are bikes stolen by petty thieves, but also by organized gangs that take many expensive bikes abroad. Many victims only report the theft because their insurance requires it, and insurers are now questioning if it is still possible to offer bike theft insurance [3].

Researchers also looked at how bike theft affects people emotionally. Half of the victims said they were very attached to their bikes and would rather get their stolen bike back than a replacement. Because of fear of theft, many people end up buying cheaper bikes or even stop using their bikes altogether. About one in five cyclists are now too afraid to take their bikes out, whether or not they've been victims of theft themselves [3].

Bike theft is a widespread problem in the Netherlands. Experts estimate that more than 750,000 bikes are stolen every year, but the real number is probably higher since many people do not report the theft. Big cities like Amsterdam, Utrecht, and Rotterdam are known for having a high risk of bike theft. The growing popularity of electric bikes, cargo bikes, and fast e-bikes has made stealing bikes even more tempting for criminals [4].

Despite these problems, cycling is a key part of life in the Netherlands. There are around 23 million bikes for the country's 17 million people. Bicycles are a major way to get around, especially for short trips in cities, and they account for more than a quarter of all travel in the country. The Netherlands also has an excellent cycling infrastructure, with about 35,000 kilometers of bike paths connecting cities and towns, which makes biking easy and enjoyable for commuting and leisure [5]. Even if you use strong locks and stay careful, many bike thieves are skilled and act quickly. The police and local governments are trying hard to stop them, but the chances of actually catching these thieves are very small.

B. Statement of Problem

It is very difficult to detect bike theft when someone lifts the bike into a car or tilts it into a van without accidentally

triggering false alarms during normal use, like riding or when the owner lifts the bike onto a rack. Another big challenge is creating a real-time theft detection system that uses little power and works well with LoRa network systems. In this research, we tackled these problems by using just a 3-axis accelerometer and a custom Interval Type-2 Fuzzy Logic System (IT2FLS) to apply specific rules. Unlike systems that rely only on fixed thresholds which often give false alarms because of small bumps, our system is designed to handle sensor noise and normal movements, yet still detect suspicious lifting patterns. We focused especially on lift-related theft actions and tested our system with different real-life scenarios, including both actual thefts and harmless situations, to make sure it accurately tells the difference without too many false alarms.

C. Requirements

The system must meet the following requirements:

- **Low false alarm rate:** Keep false alarms below 5% based on labeled test data, meaning it should reduce false positives by at least 95%.
- **Battery life:** The battery should last at least five years with normal use, assuming two rides per day.
- **LoRa compatibility:** The system must work within the current data transmission limits of the LoRa network.
- **Single sensor dependence:** It should rely only on data from the existing accelerometer, without needing extra sensors.
- **Operational reliability:** Keeping false positives under 5% is crucial so the system does not cause unnecessary maintenance or service calls.

D. Research Questions

The aim of this work is to create an intelligent e-bike theft detection system using an Interval Type-2 Fuzzy Logic System (IT2FLS). To achieve this, the following research questions will be answered:

1) Which sensor features derived from accelerometer signals are most useful for accurately detecting theft-like events?
2) How well can a fuzzy inference system based on accelerometer data tell the difference between theft and non-theft situations in e-bikes?
3) Can interval type-2 fuzzy sets make theft detection more reliable by handling sensor noise and uncertainty better?
4) What risk score best balances sensitivity (catching real thefts) and specificity (avoiding false alarms) in the fuzzy decision-making system?
5) Is it possible to build the system in a way that uses little battery power and can be easily added to real e-bikes using embedded hardware?
6) Which motion features such as lift acceleration, pedal stillness, tilt, Z-orientation, or car-like movement, are most effective for spotting theft in real-world scenarios?

II. Literature Review

This section explains the sensor device, the people involved in the project, and the method used to build the intelligent theft detection system with Interval Type-2 Fuzzy Logic.

A. Accelerometer Sensor

An accelerometer is a sensor that measures how quickly something speeds up or slows down, helping to track movements over time [6]. It reports these changes in acceleration in units of g. Although some accelerometers can measure movement in only one or two directions, most models today measure in three directions (triaxial). The popularity of smartphones has made accelerometers very common since almost all modern phones include a triaxial accelerometer, and many also have gyroscopes and magnetometers [7]. In this research, we used a three-axis (x, y, z) accelerometer provided by our partners, Bowtag and Bypoint, as the main sensor for detecting theft-related motions. A sample of the recorded sensor data is shown in Table I.

Table I: Example of Accelerometer Sensor Data Collected for Theft Detection

Time	ax	ay	az
06-09-2025 21:23:32.483	0.019764	-0.066612	1.003572
06-09-2025 21:23:32.493	0.023180	-0.068564	1.001620
06-09-2025 21:23:32.503	0.020008	-0.067588	1.004548

B. Sensor Device

The 4799 StreamLine LoRa FSK Security Tag, shown in Figure 1, is a reliable tracking device equipped with a tamper detection strip, making it perfect for securing valuable assets even in harsh environments. This small, lightweight tag (57 $\times$ 35 $\times$ 15 mm, only 40 grams) is sealed to meet IP68 standards, protecting it against water, dust, impacts, and extreme temperatures from -20°C to +60°C. It uses LoRa technology at EU-868 MHz for long-range communication and supports private LoRa networks or Helium, while also using FSK signals for close-range, precise positioning during recovery.

The tag includes a 3D accelerometer that can sense very light vibrations (as small as 0.016 g) up to strong movements of 16 g, with sensitivity adjustable remotely over-the-air. It also features a 700 mAh battery, allowing operation for up to seven years depending on usage settings. If the device is dislodged from where it is mounted, the tamper strip immediately triggers a user-defined alarm mode, such as sending more frequent LoRa messages or a local signal detectable by a StreamLine Scanner. The module's settings and firmware can be updated remotely, and its compatible with third-party network systems, making it a flexible solution for many security applications.

C. BouwTag and Bypoint

BouwTag and Bypoint are two innovative companies working together to make tracking and protecting valuable items easier and smarter. BouwTag is a developer and distributor of

Figure 1: 4799 StreamLine LoRa FSK Security Tag with Tamper Detection Strip

Track and Trace devices for the construction and infrastructure industries. Their products help construction companies keep track of materials, tools, and equipment on large job sites, which reduces losses and improves efficiency. BouwTag designs devices with long battery life, durable enclosures, and advanced features like temperature and movement sensors. Their website highlights solutions for asset tracking, theft prevention, and improving logistics in construction projects [8].

Bypoint, on the other hand, focuses on cycling safety and security. They develop and distribute high-quality cycling accessories and advanced tracking solutions designed to protect cyclists and their bikes from theft. Bypoint collaborates with leasing bike companies, fleet managers, and insurance providers to offer e-bike tracking systems that make bikes safer for both individual users and professional fleets [9]. Together, BouwTag and Bypoint are working on a new device that may use a complete chipset capable of collecting detailed data on temperature, movement, and location, helping customers track their assets or bikes in real time. The device is designed for long battery life of up to five years, and integrates easily into existing management systems.

D. Fuzzy Logic and Fuzzy Sets

Fuzzy logic is a way of reasoning that works with uncertain or imprecise information by assigning degrees of membership between 0 and 1, instead of only true or false [10]. For example, instead of labeling 17°C as just "cold" or "warm," fuzzy logic can say it belongs 80% to "cold" and 20% to "warm," which allows smoother adjustments in situations like controlling a heater [11].

Let's consider a set X containing elements x. In this set, a fuzzy set A is defined by a membership function $f_A(x)$ that gives each element a value between 0 and 1, called the grade of membership. The closer $f_A(x)$ is to 1, the more x belongs to A. When A is a normal (crisp) set, the membership is either 0 or 1, just like traditional yes/no logic [11].

Some important properties of fuzzy sets are [11]:

- **Emptiness:** A set A is empty on X if and only if $f_A(x) = 0$.
- **Equality:** Two sets A and B are equal if $f_A(x) = f_B(x)$ for every x in X.
- **Complementarity:** The complement of A is denoted A' and is given by $f_{A'}(x) = 1 - f_A(x)$.
- **Containment:** A is contained in B if $f_A(x) \leq f_B(x)$.
- **Union:** The union of A and B gives set C with $f_C(x) = \max(f_A(x), f_B(x))$.
- **Intersection:** The intersection of A and B gives set C with $f_C(x) = \min(f_A(x), f_B(x))$.

Fuzzy logic provides a flexible way of modeling uncertainty and gradual transitions, making it suitable for applications such as theft detection in e-bikes, where precise thresholds often fail due to noise and imprecise signals [11].

E. Fuzzy Inference Systems (FIS)

Fuzzy inference systems (FIS) use fuzzy logic rules to reach conclusions from given information. Unlike classical logic, FIS can use many different ways to connect rules (such as different types of implications or combinations), allowing a wide variety of inference methods [12]. Figure 2 shows how a fuzzy inference system works, where inputs are fuzzified, processed by an inference engine using rules, and then defuzzified to produce a clear output [13].

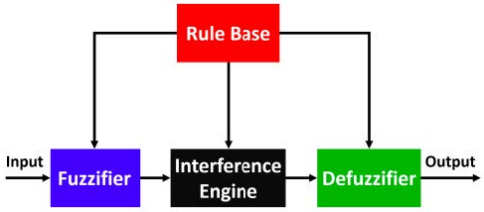

Figure 2: Fuzzy Logic Architecture

Among the common types of FIS are Mamdani and TSK systems, which are popular because they balance simplicity and performance. To understand how FIS works, it is important to know the concepts of T-norms, T-conorms, and fuzzy implications [12]:

T-norm: A T-norm $T : [0,1] \times [0,1] \to [0,1]$ combines two fuzzy membership values and satisfies:

- **Boundary:** $T(x,1) = x$ and $T(1,x) = x$
- **Monotonicity:** If $x_1 \leq x_2$ and $y_1 \leq y_2$, then $T(x_1,y_1) \leq T(x_2,y_2)$
- **Commutativity:** $T(x_1,x_2) = T(x_2,x_1)$
- **Associativity:** $T(x_1,T(x_2,x_3)) = T(T(x_1,x_2),x_3)$

T-conorm: A T-conorm $S : [0,1] \times [0,1] \to [0,1]$ is defined by [14]

$$S(x,y) = 1 - T(1-x, 1-y), \tag{1}$$

which works as the fuzzy "or" operation.

Fuzzy Implication: A fuzzy implication $I : [0,1]^2 \to [0,1]$ satisfies:

- If $x_1 \leq x_3$, then $I(x_1,x_2) \geq I(x_3,x_2)$ for all $x_1,x_2,x_3 \in [0,1]$
- If $x_2 \leq x_3$, then $I(x_1,x_2) \leq I(x_1,x_3)$
- $I(0,0) = 1$ (falsity implies anything)
- $I(1,1) = 1$ (anything implies itself)
- $I(1,0) = 0$ (Boolean logic property)

These definitions form the foundation for designing FIS that can make decisions with uncertain or imprecise data [11].

F. Interval Type-2 Fuzzy System

A Type-2 fuzzy system builds on a Type-1 system by adding another layer of uncertainty. In a Type-2 system, the membership function itself is fuzzy, so the degree of membership can vary within a range instead of being a single fixed value [15]. A Type-2 fuzzy set $\tilde{A}$ is defined as [16]:

$$\tilde{A} = \{(x, \mu_{\tilde{A}}(x,u)) \mid x \in X, u \in [0,1]; \mu_{\tilde{A}}(x,u) \in [0,1]\}, \tag{2}$$

where $\mu_{\tilde{A}}(x,u)$ shows the membership grade for an input x and a secondary membership u. The range of these possible membership values forms what is called the footprint of uncertainty (FOU), which lets Type-2 fuzzy systems describe uncertainty more accurately than Type-1 systems.

For example, a rule in a Type-2 fuzzy system might state: "IF Speed is roughly high AND Pressure is uncertain medium THEN Output is roughly high." This approach makes Type-2 systems better at dealing with noise, variability, and high uncertainty. However, because they require extra calculations for these secondary memberships, Type-2 systems are more complex and need more computational power than Type-1 systems [11].

G. Review of Similar Works

Some recent works are reviewed in the course of this research. A fuzzy logic system (FLS) combined with text-mining techniques was proposed in [17] to detect identity theft in social networks by analyzing users' language patterns, login locations, and messaging behaviours. This system estimated the likelihood of impersonation, offering a flexible detection approach adaptable to multiple social platforms.

Authors in [18] introduced an integrated anti-theft bicycle lock system combining accelerometer and gyroscope data to detect unauthorized motion. The system included a unique voltage generator capable of delivering an electric shock as an active deterrent, alongside alarms and SMS notifications, significantly enhancing protection against theft and tampering in bike-sharing environments.

A security system for electric bikes that integrates GPS and biometric authentication was developed in [19]. Their design used fingerprint-based access control coupled with real-time tracking via GSM, addressing limitations of mechanical locks. The system was validated in controlled environments and showed promise for fleet management and theft prevention applications.

Researchers designed an intrusion detection system for smart autonomous e-bikes [20], combining the Snort intrusion detection system (IDS) for network-level detection and anomaly detection for physical tampering. Their solution integrated machine learning classifiers trained on CICIDS-2017 data, demonstrating the importance of protecting both network communication and physical components of smart e-bikes.

A SVM-based predictive model combined with IoT tracking to enhance security in bike-sharing systems was introduced in [21]. By analyzing historical theft data, the model forecasted theft risks based on spatio-temporal patterns. IoT-enabled tracking devices were deployed to provide real-time location updates, proving effective in simulations and field tests at reducing theft in urban bike-sharing schemes.

Authors of [22] proposed a fuzzy logic-based IDS for autonomous vehicles, focused on detecting Denial of Service (DoS) attacks targeting vehicle communication layers. Their system achieved good detection rate with low computational cost, highlighting the applicability of fuzzy logic for precise, lightweight cyberattack detection in safety-critical vehicular systems.

Despite commendable progress in the literature, many solutions still rely on rigid thresholding, limited sensor types, or fixed scenarios, making them susceptible to false alarms during normal activities like lifting or parking. Others focus solely on network-based security or use binary logic, which may lack nuance when interpreting real-world sensor data with inherent noise and variability. By employing an interval type-2 fuzzy inference system (IT2FLS) that fuses accelerometer features such as lift acceleration, tilt, pedal stillness, and car motion, our proposed method introduces robust uncertainty handling and flexible decision boundaries.

III. Method

This section describes how the Interval Type-2 Fuzzy Logic System (IT2FLS) was developed and implemented for detecting bike theft. First, accelerometer data were collected along the X, Y, and Z axes. In this study, three potential theft scenarios are considered:

- **Scenario 1:** Bike stolen, lifted into a car trunk, and laid sideways.
- **Scenario 2:** Bike stolen, lifted upright in a trunk using its kickstand.
- **Scenario 3:** Bike stolen and hung vertically on a car's rear bumper.

A. Data Collection

Accelerometer readings were gathered from the assigned sensor at a sampling rate of 25 Hz, which allowed events to be segmented over time. Using time stamps was important to properly slide the analysis window and to compare movement patterns before and after lifting events.

The developed model relied on onboard accelerometer data to track pedal movement and detect suspicious actions such as lifting the bike or placing it in a car trunk. This approach focused specifically on the real-world theft scenarios listed above.

Features were extracted using time windows. Sequences of sensor readings were processed with a sliding window average for the X, Y and Z axes. Each function calculated a specific feature, such as pedal stillness, car motion, lift acceleration, or lift orientation. For convenience, the mean values of X, Y, and Z were also stored in each window so they could be reused for other calculations if needed. Five main input features were integrated into the system, as shown in Figure 3.

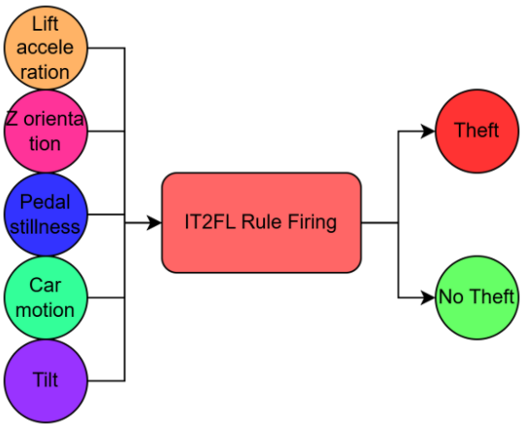

Figure 3: Main input features extracted from accelerometer data: pedal stillness, car motion, lift acceleration, lift orientation, and Z-axis orientation.

1) Lift Acceleration: For each window of N samples from the Z-axis accelerometer data, the lift acceleration L is calculated as

$$L = \max_{i=1}^{N} \left(|Z_i| \right), \tag{3}$$

which finds the highest absolute value of Z acceleration within the time window. The lift acceleration focuses on sudden movements, such as sharp spikes or large changes in the Z-axis, which can occur when a bike is lifted.

By using the maximum Z value in the window, the system can catch recent lift events even if the bike has already settled into a new position afterward. This ensures that possible theft scenarios are not missed just because the bike has stabilized during the final samples of the window.

2) Z Orientation: The Z-axis value is used as an extra clue to determine the bike's orientation. When the bike is laid sideways, the Z value typically drops sharply, which helps the system distinguish whether the bike is upright, sideways, or being lifted. By including Z orientation, the detection accuracy improves because the system can better identify these static states.

To calculate the Z orientation, the system computes the average of the Z values within each time window:

$$Z_{\text{orientation}} = \frac{1}{N} \sum_{i=1}^{N} Z_i, \tag{4}$$

where $Z_{\text{orientation}}$ represents the mean Z value in the window, providing a reliable estimate of the bike's current position.

3) Pedal Stillness: When someone is pedaling, the bike produces a repeating signal in the accelerometer data, usually in the 1–2 Hz range, matching typical pedaling speeds. A low pedal stillness value (near 0) indicates low variance, meaning the pedals are not moving and the bike may be stationary—possibly inside a car trunk. Conversely, a high value indicates significant movement, suggesting the bike is being ridden or moved.

However, pedaling does not always create a clear signal, especially if the rider changes speed frequently or if there is noise in the data. To address this, we calculated the mean absolute deviation (MAD) of a high-pass filtered signal. The high-pass filter was defined by the second-order Butterworth filter parameters:

$$b, a = \text{butter}(2, 0.7/(\text{sample\_rate}/2), \text{btype} = \text{'high'}), \tag{5}$$

which removes slow changes and emphasizes faster, pedal-related variations. The MAD of the high-pass filtered X and Y signals was then computed over a 2-second sliding window. This approach makes it easier to determine if the bike is being pedaled or not, as illustrated in Figure 4, which shows the pedal stillness computation process.

4) Car Motion: Car motion quantifies the overall movement of the bike, particularly the horizontal drifting that occurs when a bike is transported in a vehicle. To measure this, the mean absolute deviation (MAD) of the differences between consecutive X and Y accelerometer readings is calculated over a 3-second sliding window, without applying any filtering. The car motion is defined as:

$$\text{CarMotion} = \text{MAD} \left(\Delta X_i, \Delta Y_i \right), \tag{6}$$

where ΔX_i and ΔY_i are the differences between consecutive X and Y samples, respectively.

This approach helps identify smooth, continuous movement, which is indicative of the bike being inside a moving vehicle. The complete process is illustrated in Figure 5, which shows the car motion computation flowchart.

5) Tilt: Tilt is included as a fuzzy input because the bike's angle provides a strong clue about how it is being handled. By incorporating tilt, the system can better distinguish between scenarios such as the bike being upright, laid sideways, or lifted. This enables writing rules specifically for orientation-based theft patterns, which helps lower false alarms and improve detection accuracy.

To calculate tilt, the maximum absolute tilt in a window is used, based on the averaged X and Y accelerations:

$$\hat{T} = \max \left(|X|, |Y| \right), \tag{7}$$

where $X = \text{freeAccX}$ and $Y = \text{freeAccY}$. This approach ensures that the tilt calculation remains stable and reliable over recent samples.

B. Implemented Membership Functions

In this work, triangular and trapezoidal membership functions (MFs) were used to define the fuzzy input sets [23], [24].

- Triangular Membership Function
  A triangular MF $\mu(x; a, b, c, h)$ has a base from a to c, a peak at b, and a maximum height h. It is defined as

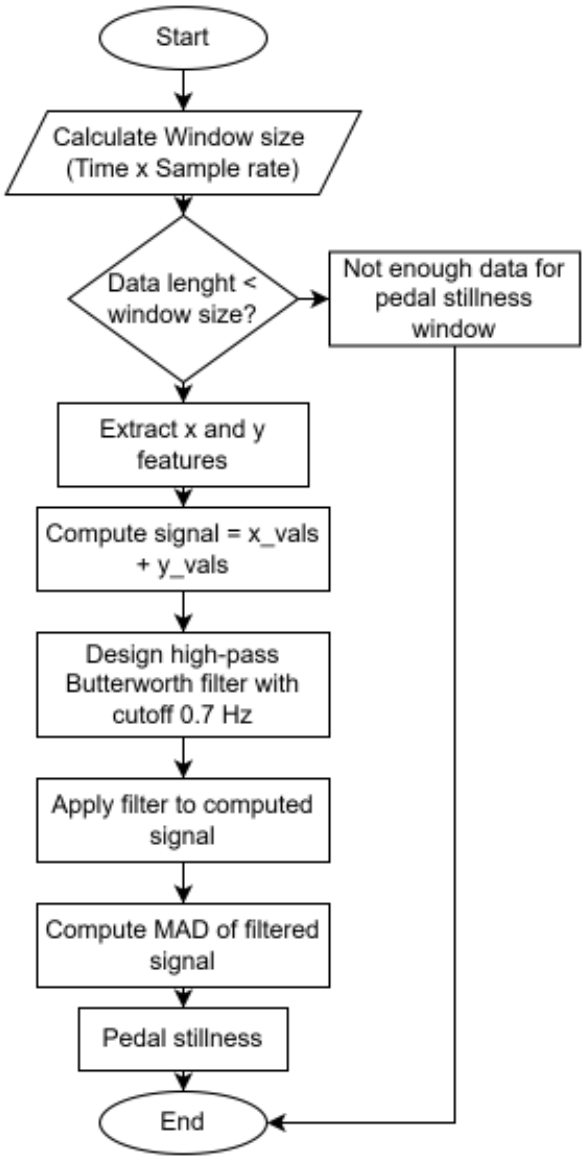

Figure 4: Flowchart for computing pedal stillness: raw signal, high-pass filtered signal, and resulting mean absolute deviation (MAD).

$$\mu(x) = h \times \begin{cases} 0, & x \le a \text{ or } x \ge c \\ \dfrac{x-a}{b-a}, & a < x < b \\ \dfrac{c-x}{c-b}, & b \le x < c \end{cases}$$

where x is the input variable.

- Trapezoidal Membership Function
  A trapezoidal MF $\mu(x; a, b, c, d, h)$ has a rising edge from a to b, a flat top between b and c, and a falling edge from c to d. It is defined as

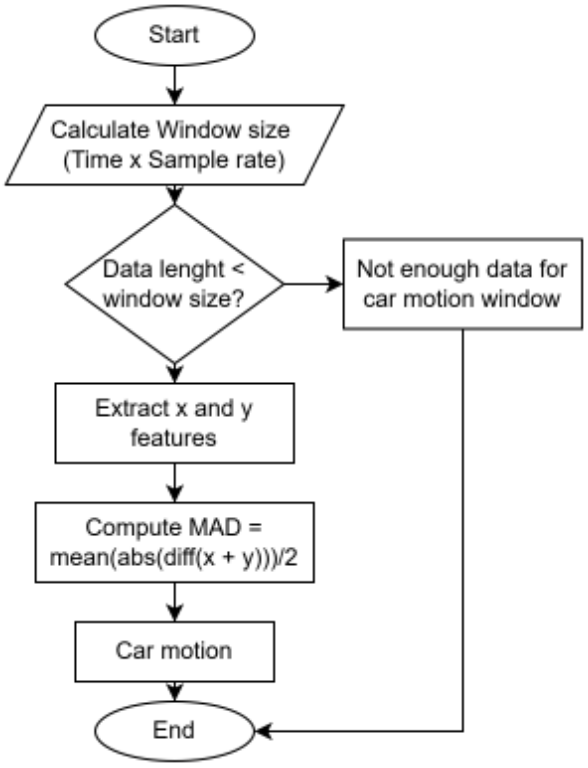

Figure 5: Flowchart of the car motion computation process: detecting smooth, ongoing movement characteristic of a bike being transported in a car.

$$\mu(x) = h \times \begin{cases} 0, & x \le a \text{ or } x \ge d \\ \dfrac{x-a}{b-a}, & a < x < b \\ 1, & b \le x \le c \\ \dfrac{d-x}{d-c}, & c < x < d \end{cases}$$

These functions allow the fuzzy system to smoothly represent different input conditions, such as low, medium, or high sensor values, which improves detection accuracy [24].

1) Lift Acceleration Membership Functions: The Lift Acceleration input is divided into three fuzzy sets: *lift_low*, *lift_normal*, and *lift_high*, each defined by lower and upper membership functions (MFs) as follows:

a) Input lift_low::

- Lower MF: triangular with $a = 0.71$, $b = 0.8$, $c = 0.9$, $h = 1.0$
- Upper MF: triangular with $a = 0.7$, $b = 0.85$, $c = 0.95$, $h = 0.8$

b) Input lift_normal::

- Lower MF: trapezoidal with $a = 0.9$, $b = 0.99$, $c = 1.1$, $d = 1.2$, $h = 1.0$
- Upper MF: trapezoidal with $a = 0.85$, $b = 0.99$, $c = 1.15$, $d = 1.25$, $h = 0.8$

c) Input lift_high::

- Lower MF: trapezoidal with $a = 1.2$, $b = 1.2$, $c = 8.0$, $d = 9.0$, $h = 1.0$
- Upper MF: trapezoidal with $a = 1.15$, $b = 1.15$, $c = 8.0$, $d = 9.0$, $h = 0.8$

Figures 6, 7, and 8 show the membership plots for *Lift low*, *Lift normal*, and *Lift high*, respectively.

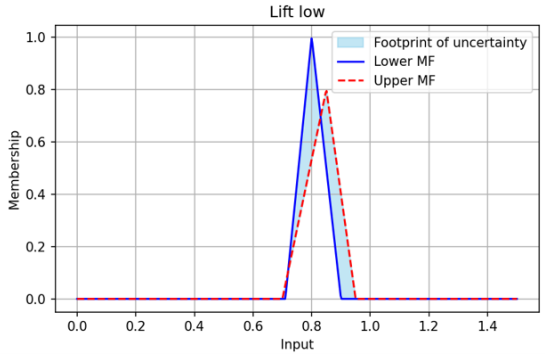

Figure 6: Membership functions for Lift Low input.

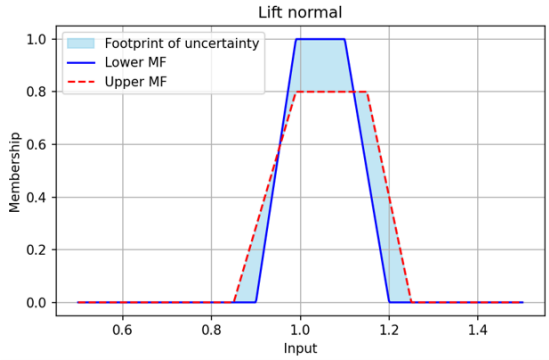

Figure 7: Membership functions for Lift Normal input.

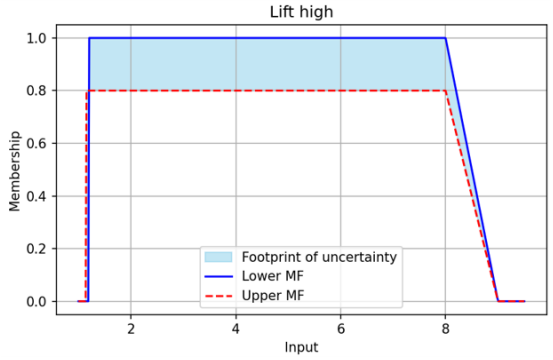

Figure 8: Membership functions for Lift High input.

2) Z Orientation Membership Functions: The Z Orientation input is divided into three fuzzy sets: *z_normal*, *z_laid*, and *z_lift*, each defined by lower and upper membership functions (MFs) as follows:

a) Input z_normal::

- Lower MF: trapezoidal with $a = 0.9$, $b = 0.95$, $c = 1.0$, $d = 1.02$, $h = 1.0$
- Upper MF: trapezoidal with $a = 0.88$, $b = 0.93$, $c = 1.01$, $d = 1.04$, $h = 0.8$

b) Input z_laid::

- Lower MF: trapezoidal with $a = 0$, $b = 0$, $c = 0.45$, $d = 0.75$, $h = 1.0$
- Upper MF: trapezoidal with $a = 0$, $b = 0$, $c = 0.5$, $d = 0.78$, $h = 0.8$

c) Input z_lift::

- Lower MF: trapezoidal with $a = 1.2$, $b = 1.3$, $c = 5.5$, $d = 6.0$, $h = 1.0$
- Upper MF: trapezoidal with $a = 1.15$, $b = 1.25$, $c = 5.8$, $d = 6.2$, $h = 0.8$

3) Pedal Stillness Membership Functions: The Pedal Stillness input is divided into two fuzzy sets: *pedal_still_low* and *pedal_still_high*, each defined by lower and upper membership functions (MFs) as follows:

a) Input pedal_still_low::

- Lower MF: trapezoidal with $a = 0$, $b = 0$, $c = 0.04$, $d = 0.06$, $h = 1.0$
- Upper MF: trapezoidal with $a = 0$, $b = 0$, $c = 0.05$, $d = 0.07$, $h = 0.8$

b) Input pedal_still_high::

- Lower MF: trapezoidal with $a = 0.06$, $b = 0.08$, $c = 0.5$, $d = 0.5$, $h = 1.0$
- Upper MF: trapezoidal with $a = 0.05$, $b = 0.07$, $c = 0.5$, $d = 0.5$, $h = 0.8$

4) Car Motion Membership Functions: The Car Motion input is divided into two fuzzy sets: *motion_static* and *motion_moving*, each defined by lower and upper membership functions (MFs) as follows:

a) Input motion_static::

- Lower MF: trapezoidal with $a = 0$, $b = 0$, $c = 0.01$, $d = 0.043$, $h = 1.0$
- Upper MF: trapezoidal with $a = 0$, $b = 0$, $c = 0.02$, $d = 0.0435$, $h = 0.8$

b) Input motion_moving::

- Lower MF: trapezoidal with $a = 0.044$, $b = 0.044$, $c = 0.1$, $d = 0.2$, $h = 1.0$
- Upper MF: trapezoidal with $a = 0.043$, $b = 0.04$, $c = 0.15$, $d = 0.25$, $h = 0.8$

5) Tilt Membership Functions: The Tilt input is divided into two fuzzy sets: *tilt_low* and *tilt_high*, each defined by lower and upper membership functions (MFs) as follows:

a) Input tilt_low::

- Lower MF: trapezoidal with $a = 0$, $b = 0$, $c = 0.005$, $d = 0.0085$, $h = 1.0$
- Upper MF: trapezoidal with $a = 0$, $b = 0$, $c = 0.004$, $d = 0.0085$, $h = 0.8$

b) Input tilt_high::

- Lower MF: trapezoidal with $a = 0.009$, $b = 0.01$, $c = 0.03$, $d = 0.5$, $h = 1.0$
- Upper MF: trapezoidal with $a = 0.0085$, $b = 0.01$, $c = 0.04$, $d = 0.6$, $h = 0.8$

6) Output Risk Membership Functions: The Output Risk variable is divided into three fuzzy sets: *risk_low*, *risk_medium*, and *risk_high*, each defined by lower and upper membership functions (MFs) as follows:

a) Output risk_low::

- Lower MF: triangular with $a = 0$, $b = 0$, $c = 40$, $h = 1.0$
- Upper MF: triangular with $a = 0$, $b = 0$, $c = 60$, $h = 0.8$

b) Output risk_medium::

- Lower MF: trapezoidal with $a = 20$, $b = 50$, $c = 70$, $d = 90$, $h = 1.0$
- Upper MF: trapezoidal with $a = 10$, $b = 40$, $c = 80$, $d = 100$, $h = 0.8$

c) Output risk_high::

- Lower MF: triangular with $a = 60$, $b = 100$, $c = 100$, $h = 1.0$
- Upper MF: triangular with $a = 40$, $b = 100$, $c = 100$, $h = 0.8$

All figures showing the membership plots for z orientation, pedal stillness, car motion, tilt and risk output are given in the Appendix.

C. Fuzzy Inference Rule Firing

All fuzzy logic calculations in this system were built entirely from scratch. The output of the fuzzy system is given as a risk percentage, which is determined through interval centroid defuzzification. In this method, all active (or "fired") fuzzy rules contribute to the centroid calculation, with each rule's output weighted by its lower and upper firing strengths, resulting in an accurate interval centroid estimate.

Multiple rules can fire simultaneously for a single input. To generate a realistic output shape, each rule's result is sampled at multiple points, and the final risk score is calculated as the weighted average of all these fired outputs.

The fuzzy rules are organized in several tables. Table II shows the fuzzy rules for **Scenario 1: bike laid sideways**. Table III shows the rules for **Scenario 2: bike upright in a car trunk**. Table IV covers **Scenario 3: bike hung vertically on a car rear bumper**. Table V includes the rules for **low-risk situations and catch-all cases**.

These rules are designed so that those with significant firing strength correspond to high and medium risk scenarios. They cover major combinations like high lift acceleration with low pedal movement and car motion, to accurately detect theft. The rules also help avoid false positives by distinguishing normal bike rack lifts from actual theft by checking for the presence of car-like motion. This ensures the system can reliably detect different types of theft, including sideways, upright, and hanging scenarios.

IV. Results

This section presents and analyzes the results of the project. All code was written in Python and executed on an HP laptop with an Intel Core i5 processor, 16 GB of RAM, and a 2.3 GHz processing speed. The developed algorithm was tested and validated using five real-world bike theft scenarios to assess its performance and accuracy.

A. Scenario 1: Bike Hung Vertically on Rear Bumper (True Positive)

Figure 9: Scenario 1: Bike hung vertically on rear bumper.

In this case, the result showing a defuzzified risk of 60.73% correctly exceeds the 60% threshold, leading the fuzzy system to detect theft. This aligns with the scenario shown in Figures 9, where the bike is on a thief's car, confirming that the algorithm successfully identified the suspicious lifting and motion patterns as an actual theft event.

B. Scenario 2: Bike Lifted to Upper Parking Rack (False Positive)

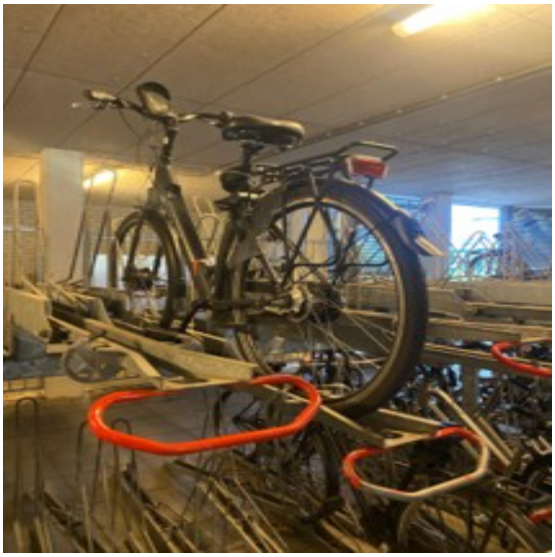

Figure 10: Scenario 2: Bike lifted to upper parking rack.

In this result, the IT2FLS computed a defuzzified risk of 43.69%, which is below the 60% threshold, leading it to classify the situation as "No theft." This matches the real

Table II: Fuzzy rules for Scenario 1: Bike laid sideways

S/N	Rule	Theft Risk
1	Tilt = High AND Z-Orientation = Laid	Medium
2	Lift Acceleration = High AND Z-Orientation = Laid	Medium
3	Lift Acceleration = High AND Z-Orientation = Tilt High	Medium
4	Lift Acceleration = High AND Tilt = High AND Car Motion = Moving	Medium
5	Lift Acceleration = High AND Tilt = High AND Pedal Stillness = Low	Medium
6	Lift Acceleration = High AND Z-Orientation = Laid AND Tilt = High AND Car Motion = Static AND Pedal Stillness = Low	Medium
7	Lift Acceleration = High AND Tilt = High AND Car Motion = Moving AND Pedal Stillness = Low	High
8	Lift Acceleration = High AND Z-Orientation = Laid AND Tilt = High AND Car Motion = Moving AND Pedal Stillness = Low	High

Table III: Fuzzy rules for Scenario 2: Bike upright in car trunk

S/N	Rule	Theft Risk
1	Lift Acceleration = High AND Tilt = Park AND Car Motion = Moving	Medium
2	Lift Acceleration = High AND Z-Orientation = Lift AND Tilt = Park AND Car Motion = Static AND Pedal Stillness = Low	Medium
3	Lift Acceleration = High AND Tilt = Park AND Car Motion = Moving AND Pedal Stillness = Low	High
4	Lift Acceleration = High AND Z-Orientation = Lift AND Tilt = Park AND Car Motion = Moving AND Pedal Stillness = Low	High

Table IV: Fuzzy rules for Scenario 3: Bike hung vertically on car rear bumper

S/N	Rule	Theft Risk
1	Lift Acceleration = High AND Z-Orientation = Normal AND Car Motion = Moving AND Pedal Stillness = Low	Medium
2	Lift Acceleration = Normal AND Z-Orientation = Lift AND Car Motion = Moving AND Pedal Stillness = High	Medium
3	Lift Acceleration = High AND Z-Orientation = Lift AND Car Motion = Static AND Pedal Stillness = Low	Medium
4	Lift Acceleration = High AND Car Motion = Moving AND Pedal Stillness = Low	High
5	Lift Acceleration = Normal AND Z-Orientation = Lift AND Car Motion = Moving AND Pedal Stillness = Low	High
6	Lift Acceleration = Normal AND Tilt = Park AND Car Motion = Moving	Medium

Table V: Fuzzy rules for low-risk situations and catch-all cases

S/N	Rule	Theft Risk
1	Lift Acceleration = High AND Tilt = High AND Car Motion = Static	Low
2	Lift Acceleration = High AND Tilt = Park AND Car Motion = Static	Low
3	Lift Acceleration = Low AND Car Motion = Static	Low
4	Lift Acceleration = Low AND Car Motion = Moving	Low
5	Lift Acceleration = High AND Pedal Stillness = High (normal bike riding)	Low
6	Lift Acceleration = Normal AND Pedal Stillness = High (normal bike riding)	Low

Table VI: Fuzzy inference results for Scenario 1

Input Variable	Value	Memberships & Ranges
lift_accel	1.508	Low: 0.00–0.00, Normal: 0.00–0.00, High: 1.00–0.80
pedal_stillness	0.055	Low: 0.24–0.59, High: 0.00–0.21
car_motion	0.044	Static: 0.00–0.00, Moving: 1.00–0.80
tilt	0.200	Park: 0.00–0.00, High: 0.64–0.57
z_orientation	0.997	Normal: 1.00–0.80, Laid: 0.00–0.00, Lift: 0.00–0.00
Defuzzified Risk	60.73%	
Detection Result	**THEFT DETECTED**	

Table VII: Fuzzy inference results for Scenario 2

Input Variable	Value	Memberships & Ranges
lift_accel	2.321	Low: 0.00–0.00, Normal: 0.00–0.00, High: 1.00–0.80
pedal_stillness	0.005	Low: 1.00–0.80, High: 0.00–0.00
car_motion	0.004	Static: 1.00–0.80, Moving: 0.00–0.00
tilt	0.179	Park: 0.00–0.00, High: 0.68–0.60
z_orientation	1.020	Normal: 0.00–0.53, Laid: 0.00–0.00, Lift: 0.00–0.00
Defuzzified Risk	43.69%	
Detection Result	**NO THEFT**	

scenario shown in Figures 10, where the bike is simply being lifted to an upper-tier parking rack, a legitimate action by the owner rather than a theft attempt. This indicates the algorithm correctly avoided a false alarm in this case, demonstrating it can distinguish normal user behavior from suspicious activity when the lift alone does not trigger high risk.

C. Scenario 3: Normal Pedal Riding by User (False Positive)

In the scenario, the IT2FLS produced a defuzzified risk of 34.05%, well below the 60% threshold, leading it to correctly classify the scenario as "No theft." This matches the real situation in Figures 11, where the user is simply pedaling the bike normally, showing a typical riding behaviour without

Figure 11: Scenario 3: Normal pedal riding by user.

suspicious patterns. This indicates the algorithm successfully avoided a false positive, recognizing standard bike use as safe and not mistaking regular pedaling for a theft event.

Table VIII: Fuzzy inference results for Scenario 3

Input Variable	Value	Memberships & Ranges
lift_accel	2.011	Low: 0.00–0.00, Normal: 0.00–0.00, High: 1.00–0.80
pedal_stillness	0.067	Low: 0.00–0.13, High: 0.34–0.67
car_motion	0.043	Static: 0.00–0.01, Moving: 0.00–0.80
tilt	0.058	Park: 0.00–0.00, High: 0.94–0.77
z_orientation	1.000	Normal: 0.98–0.80, Laid: 0.00–0.00, Lift: 0.00–0.00
Defuzzified Risk	34.05%	
Detection Result	**NO THEFT**	

D. Scenario 4: Bike Parked with Front Wheel Lifted onto Rack, Rear Wheel on Ground, Tilted Backward (False Positive)

Figure 12: Scenario 4: Bike parked with front wheel lifted onto rack, rear wheel on ground, tilted backward.

In this result, the IT2FLS computed a defuzzified risk of 43.60%, which is below the 60% threshold, so it classified the scenario as "No theft." This matches the real situation in Figures 12, where the bike's front wheel is lifted onto a rack and the bike tilts backward with the rear wheel on the ground. This is a typical parking maneuver rather than a theft attempt. The algorithm correctly recognized this legitimate action and avoided a false alarm, showing it can handle cases with brief lifting and tilt during normal parking without misclassifying them as theft.

Table IX: Fuzzy inference results for Scenario 4

Input Variable	Value	Memberships & Ranges
lift_accel	1.724	Low: 0.00–0.00, Normal: 0.00–0.00, High: 1.00–0.80
pedal_stillness	0.004	Low: 1.00–0.80, High: 0.00–0.00
car_motion	0.003	Static: 1.00–0.80, Moving: 0.00–0.00
tilt	0.200	Park: 0.00–0.00, High: 0.64–0.57
z_orientation	0.984	Normal: 1.00–0.80, Laid: 0.00–0.00, Lift: 0.00–0.00
Defuzzified Risk	43.60%	
Detection Result	**NO THEFT**	

E. Scenario 5: Bike Laid Sideways to the Ground (False Positive)

Figure 13: Scenario 5: Bike laid sideways to the ground.

In this result, the IT2FLS calculated a defuzzified risk of 56.54%, which is just below the 60% threshold, so it classified the situation as "No theft." This matches the scenario shown in Figures 13, where the bike has accidentally fallen sideways onto the ground, likely from being improperly parked or bumped, rather than an active theft. The algorithm correctly identified this as a non-theft event, avoiding a false positive despite the sudden tilt and unusual position of the bike.

F. Performance Summary

The confusion matrix in Figure 14 summarizes the system's performance in classifying theft and non-theft scenarios. The confusion matrix demonstrates the effectiveness of the fuzzy

Table X: Fuzzy inference results for Scenario 5

Input Variable	Value	Memberships & Ranges
lift_accel	1.026	Low: 0.00–0.00, Normal: 1.00–0.80, High: 0.00–0.00
pedal_stillness	0.005	Low: 1.00–0.80, High: 0.00–0.00
car_motion	0.003	Static: 1.00–0.80, Moving: 0.00–0.00
tilt	0.200	Park: 0.00–0.00, High: 0.64–0.57
z_orientation	0.258	Normal: 0.00–0.00, Laid: 1.00–0.80, Lift: 0.00–0.00
Defuzzified Risk	56.54%	
Detection Result	**NO THEFT**	

inference system on the tested cases. It shows one true positive, where the system correctly identified the theft scenario, and four true negatives, where non-theft scenarios were classified as normal behavior. There were no false positives or false negatives, resulting in perfect scores for accuracy, precision, recall, and specificity. This indicates that, within this limited test set, the system was able to perfectly distinguish between theft and non-theft events.

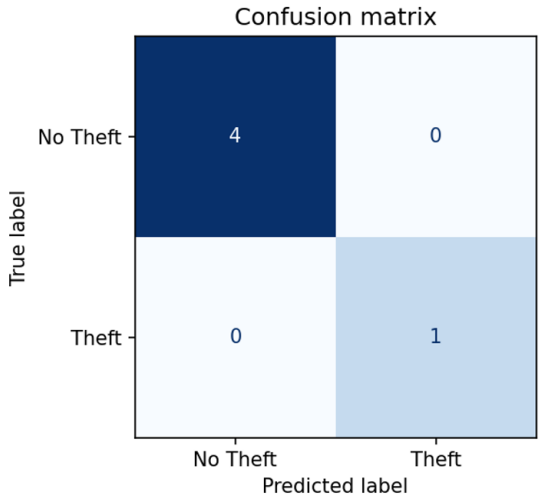

Figure 14: Confusion matrix summarizing system performance on the five tested scenarios.

The risk distribution bar plot in Figure 15 provides further insight into how the fuzzy system assessed each scenario. The plot displays the calculated defuzzified risk percentages for all five scenarios, with green bars representing non-theft cases and the red bar representing the theft case. A dashed line at the 60% risk threshold separates predictions labeled as theft from those labeled as non-theft. In this test, only the theft scenario produced a risk score above the threshold, while all normal scenarios stayed below it. This distinct separation suggests that the system is capable of differentiating theft-like events from regular activities based on sensor patterns.

G. Comparison with Type-1 Fuzzy System

We also compared our results with those from a Type-1 fuzzy system, as shown in Table XI. Using a threshold

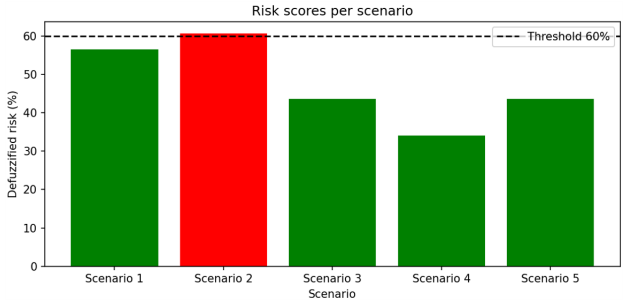

Figure 15: Risk distribution bar plot showing defuzzified risk percentages for each scenario.

where a defuzzified risk score of 60% or higher indicates theft, and below 60% indicates no theft, the Interval Type-2 Fuzzy Logic System (IT2FLS) achieved perfect accuracy by correctly classifying all five scenarios. In contrast, the Type-1 fuzzy system missed two cases (Scenarios 1 and 4) and achieved only 60% accuracy overall. This means that IT2FLS improved detection performance by 66.67% compared to the Type-1 system, demonstrating that it can handle uncertainties better and detect theft more reliably in the tested conditions.

V. Conclusion

In this project, we developed a fuzzy logic-based system to detect e-bike theft, which successfully distinguished between theft and normal bike activities in our controlled tests. The fuzzy inference system employed interval type-2 membership functions and achieved perfect performance across the five evaluated scenarios. It accurately detected theft events while avoiding false alarms during typical actions such as parking or riding. Our analysis indicated that lift acceleration and car motion were the most significant features for identifying theft. Additionally, the use of interval type-2 fuzzy sets made the system more robust to sensor noise and variable conditions, improving detection reliability. These results addressed the research questions and demonstrated that fuzzy logic is a promising approach for creating intelligent, sensor-based e-bike theft detection systems. For future work, we recommend collecting a broader dataset to confirm its effectiveness and generalizability.

CRediT Authorship Contribution Statement

Olusesi Meadows (expert in software and data engineering): wrote the Introduction, Methodology, and Results Analysis sections; reviewed the tables and figures; and checked the manuscript for grammatical accuracy.

Saman Gharagozlou (expert in machine learning): wrote the Abstract, Literature Review, and Conclusion; reviewed and edited the references to conform to IEEE standards; and checked the mathematical equations for correctness.

Appendix A
Membership Function Plots

The membership functions of pedal stillness are shown in Figures 16 and 17.

Table XI: Comparison of Type-1 and IT2FLS predictions for five test scenarios

Scenario	Type-1 Fuzzy Risk	IT2FLS Risk	Actual Detection	Type-1 Prediction	IT2FLS Prediction
1	53.67%	60.73%	Theft	No theft ($53.67 < 60$)	Theft ($60.73 \geq 60$)
2	58.01%	43.69%	No theft	No theft ($58.01 < 60$)	No theft ($43.69 < 60$)
3	47.00%	34.05%	No theft	No theft ($47.00 < 60$)	No theft ($34.05 < 60$)
4	61.00%	43.60%	No theft	Theft ($61.00 \geq 60$)	No theft ($43.60 < 60$)
5	42.83%	56.54%	No theft	No theft ($42.83 < 60$)	No theft ($56.54 < 60$)

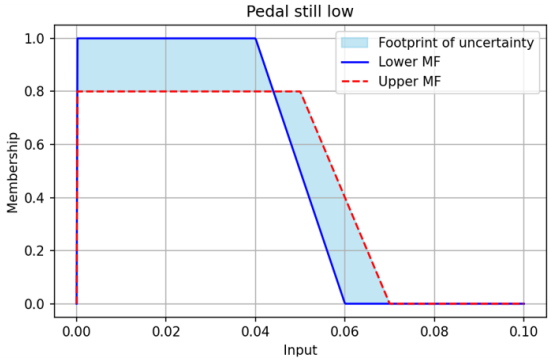

Figure 16: Membership function for pedal stillness: low.

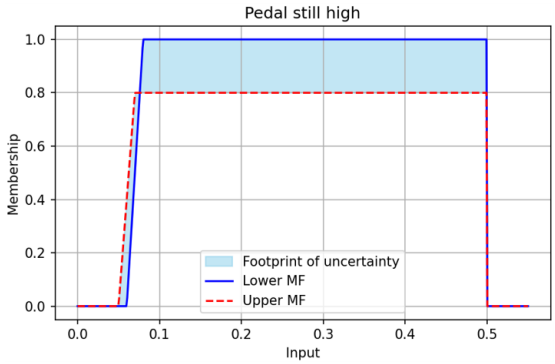

Figure 17: Membership function for pedal stillness: high.

The membership functions of car motion are shown in Figures 18 and 19.

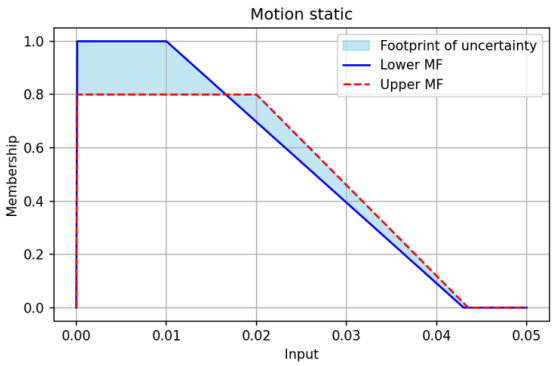

Figure 18: Membership function for car motion: static.

The membership functions of tilt are shown in Figures 20 and 21.

The membership functions of Z orientation are shown in

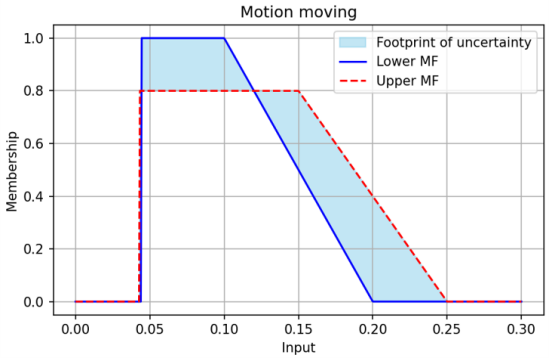

Figure 19: Membership function for car motion: moving.

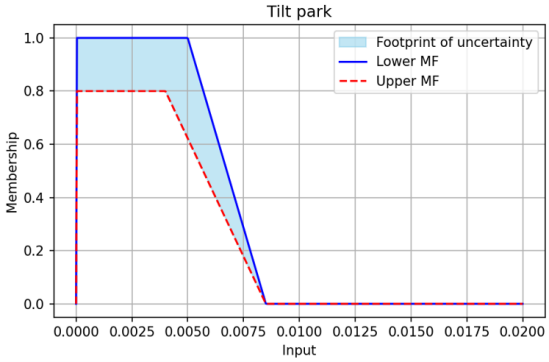

Figure 20: Membership function for tilt: park.

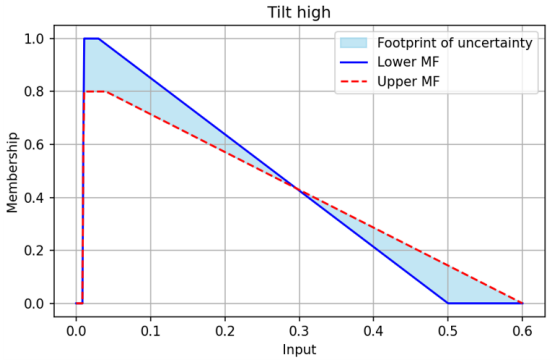

Figure 21: Membership function for tilt: high.

Figures 22, 23, and 24.

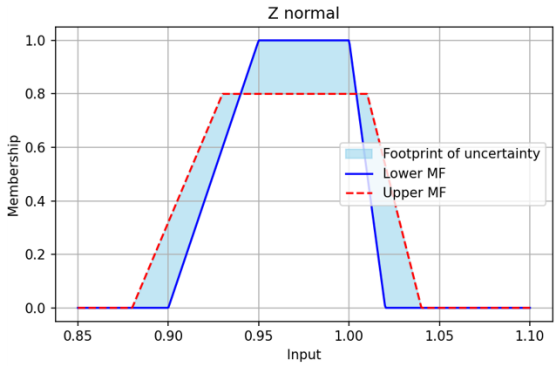

Figure 22: Membership function for Z orientation: normal.

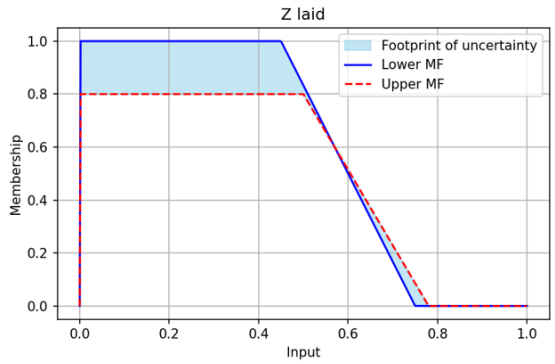

Figure 23: Membership function for Z orientation: laid.

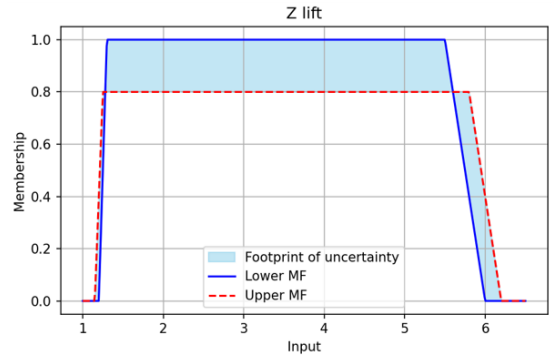

Figure 24: Membership function for Z orientation: lift.

The membership functions of the risk output are shown in Figures 25, 26, and 27.

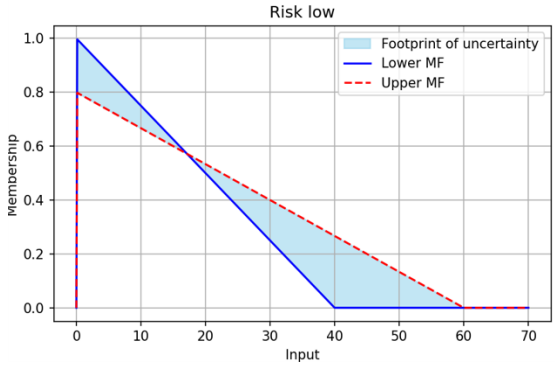

Figure 25: Membership function for risk output: low.

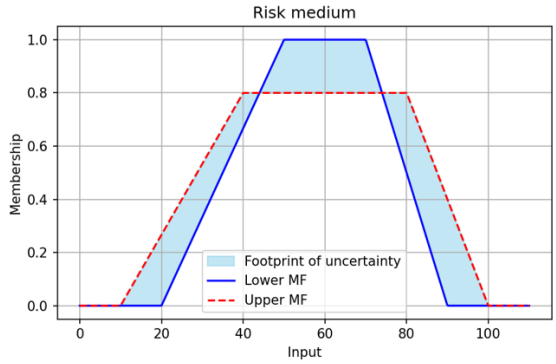

Figure 26: Membership function for risk output: medium.

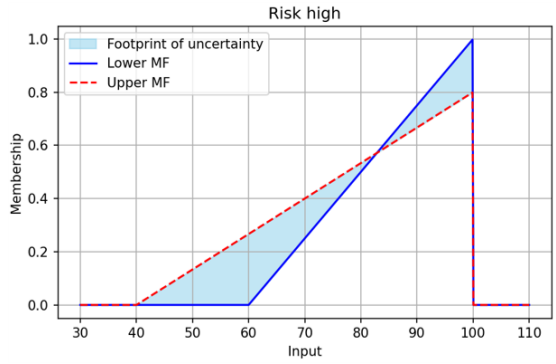

Figure 27: Membership function for risk output: high.

References

[1] J. MacArthur, J. Dill, and M. Person, "Electric bikes in north america: Results from an online survey," *Transportation Research Record: Journal of the Transportation Research Board*, vol. 2468, pp. 123–130, 2014.

[2] E. Fishman and C. Cherry, "E-bikes in the mainstream: Reviewing a decade of research," *Transport Reviews*, vol. 36, no. 1, pp. 72–91, 2016.

[3] KPN IOT. (2025) How are the dutch solving bicycle theft? with the connected bike! Accessed: 2025-06-29. [Online]. Available: https://m2m.kpn.com/en/blog/how-are-the-dutch-solving-bicycle-theft-with-the-connected-bike

[4] Bikebase. (2025) Bicycle theft in the netherlands: Facts, tips and solutions. Accessed: 2025-06-29. [Online]. Available: https://www.bikebaze.nl/en/blog/fietsdiefstal-in-nederland-feiten-tips-en-oplossingen

[5] G. of the Netherlands. (2025) Bicycles. Accessed: 2025-06-29. [Online]. Available: https://www.government.nl/topics/bicycles#:~:text=The%20Netherlands%20is%20the%20number,public%20transport%20and%20passenger%20cars.

[6] G. R. Naik, *Biomedical Signal Processing*. Springer, 2020. [Online]. Available: https://link.springer.com/book/10.1007/978-3-030-37343-5

[7] M. De Marsico and A. Mecca, "Chapter 8 - gait recognition: The wearable solution," in *Human Recognition in Unconstrained Environments*, M. De Marsico, M. Nappi, and H. Proença, Eds. Academic Press, 2017, pp. 177–195. [Online]. Available: https://www.sciencedirect.com/science/article/pii/B9780081007051000087

[8] BouwTag. (2025) Bouwtag slim materieelbeheer. Accessed: 2025-06-29. [Online]. Available: https://bouwtag.nl/

[9] Bypoint. (2025) Bypoint: The brand for innovative bicycle safety. Accessed: 2025-06-29. [Online]. Available: https://bypoint.nl/

[10] L. A. Zadeh, G. J. Klir, and B. Yuan, *Fuzzy Sets, Fuzzy Logic, and Fuzzy Systems: Selected Papers*. World Scientific, 1996, vol. 6. [Online]. Available: https://www.worldscientific.com/worldscibooks/10.1142/3132

[11] H. Ouifak and A. Idri, "A comprehensive review of fuzzy logic based interpretability and explainability of machine learning techniques across domains," *Neurocomputing*, p. 130602, 2025.

[12] U. Höhle and S. E. Rodabaugh, *Mathematics of Fuzzy Sets: Logic, Topology, and Measure Theory*. Springer Science & Business Media, 2012, vol. 3. [Online]. Available: https://link.springer.com/book/10.1007/978-94-007-0339-8

[13] Inst Tools. (2025) What is fuzzy logic? advantages, disadvantages, applications. Accessed: 2025-06-29. [Online]. Available: https://instrumentationtools.com/what-is-fuzzy-logic/

[14] M. Baczyński and B. Jayaram, "An introduction to fuzzy implications," in *Fuzzy Implications*. Springer, 2008, pp. 1–35. [Online]. Available: https://link.springer.com/chapter/10.1007/978-3-540-75765-8_1

[15] K. Mittal, A. Jain, K. S. Vaisla, O. Castillo, and J. Kacprzyk, "A comprehensive review on type-2 fuzzy logic applications: Past, present and future," *Engineering Applications of Artificial Intelligence*, vol. 95, p. 103916, 2020. [Online]. Available: https://www.sciencedirect.com/science/article/pii/S0952197620303631

[16] F. P. Nishanth, S. K. Dash, and S. R. Mahapatro, "Critical study of type-2 fuzzy logic control from theory to applications: A state-of-the-art comprehensive survey," *e-Prime - Advances in Electrical Engineering, Electronics and Energy*, p. 100771, 2024. [Online]. Available: https://www.sciencedirect.com/science/article/pii/S2772651324000030

[17] J. Á. Concepción-Sánchez, J. Molina-Gil, P. Caballero-Gil, and I. Santos-González, "Fuzzy logic system for identity theft detection in social networks," in *2018 4th International Conference on Big Data Innovations and Applications (Innovate-Data)*. IEEE, 2018, pp. 65–70.

[18] E. D. Cabalquinto, L. M. Malabayabas, K. A. A. Pulido, J. M. P. Araña, and D. J. Lopez, "Anti-theft integrated bike lock with gyroscope sensor and accelerometer motion detection," in *2022 IEEE 14th International Conference on Humanoid, Nanotechnology, Information Technology, Communication and Control, Environment, and Management (HNICEM)*. IEEE, 2022, pp. 1–6.

[19] N. Gala, A. Poswalia, and R. Gharat, "Electric bike security: Biometric & gps integration for intrusion detection," in *2023 International Conference on Sustainable Computing and Data Communication Systems (ICSCDS)*. IEEE, 2023, pp. 1618–1627.

[20] R. Maged, M. Sabry, A. Ali, I. Mesabah, A. Mazhr, and H. Soubra, "An intrusion detection system for smart autonomous e-bikes," in *2023 Eleventh International Conference on Intelligent Computing and Information Systems (ICICIS)*. IEEE, 2023, pp. 233–240.

[21] K. Karthika, A. Nithya, M. Sujatha, R. K. Kovarasan, A. Mahesh, and S. Murugan, "Advancing bike sharing security with svm and iot-enabled tracking and anti-theft measures," in *2024 2nd International Conference on Sustainable Computing and Smart Systems (ICSCSS)*. IEEE, 2024, pp. 351–356.

[22] M. Sadaf, Z. Iqbal, Z. Anwar, U. Noor, M. Imran, and T. R. Gadekallu, "A novel framework for detection and prevention of denial of service attacks on autonomous vehicles using fuzzy logic," *Vehicular Communications*, vol. 46, p. 100741, 2024. [Online]. Available: https://www.sciencedirect.com/science/article/pii/S2214209624000021

[23] MATLAB. (2025) Triangular membership function. Accessed: 2025-06-29. [Online]. Available: https://www.mathworks.com/help/fuzzy/triangularmf.html

[24] ——. (2025) Trapezoidal membership function. Accessed: 2025-06-29. [Online]. Available: https://www.mathworks.com/help/fuzzy/trapezoidalmf.html